Inhibited dynamic recovery and screw dislocation annihilation in multiple slip of FCC single crystals

Ladislas Kubin, Benoit Devincre, Thierry Hoc

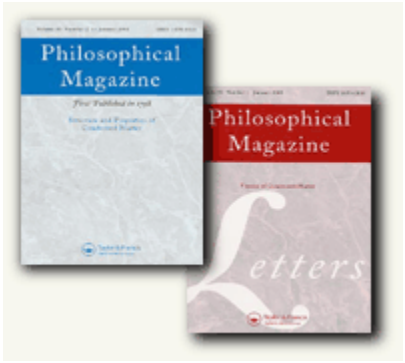

Inhibited dynamic recovery and screw dislocation annihilation in multiple slip of FCC single crystals

Journal:	*Philosophical Magazine & Philosophical Magazine Letters*
Manuscript ID:	TPHM-05-Jul-0347.R3
Journal Selection:	Philosophical Magazine
Date Submitted by the Author:	13-Dec-2005
Complete List of Authors:	Kubin, Ladislas; CNRS-ONERA, LEM Devincre, Benoit; CNRS-ONERA, LEM Hoc, Thierry; Ecole Centrale Paris, MSSMat
Keywords:	stress-strain diagram, crystals
Keywords (user supplied):	cross-slip, dynamic recovery, screw dislocations

Inhibited dynamic recovery and screw dislocation annihilation in multiple slip of FCC single crystals

L. P. KUBIN[*=], B. DEVINCRE and T. HOC[*]

Laboratoire d'Étude des Microstructures, CNRS-ONERA,

29 Avenue de la Division Leclerc, BP 72, 92322 Châtillon Cedex, France

[*]Laboratoire MSSMat, Ecole Centrale Paris, Grande Voie des Vignes,

92195 Châtenay-Malabry Cedex, France

Abstract

In face-centred cubic crystals, the stress-strain curves of <111> crystals exhibit the peculiarity of being remarkably insensitive to dynamic recovery, as compared to other orientations. This effect is attested by several early experimental studies on copper, aluminium and silver crystals. The inhibition of dynamic recovery is attributed to a reduction of the rate of annihilation of screw dislocations. The underlying mechanisms are investigated in terms of the reversal of the direction of the resolved stress in the cross-slip plane, which occurs when going from <001> to <111> orientations. Two distinct processes governing dynamic recovery in <111> crystals, acute cross-slip and backward annihilation, are examined and discussed. The second one arises because screw dislocation annihilation occurs along the direction opposite to that of the resolved applied stress in the cross-slip plane. It is concluded that, except possibly in aluminium, backward annihilation is always responsible for the inhibition of dynamic recovery in <111> crystals.

Keywords:

Cross-slip, screw dislocations, dynamic recovery, crystals, stress-strain curves

[=] Email: Ladislas.Kubin@onera.fr

1. Introduction

The present work discusses a question that arose during the modelling of strain hardening and its orientation dependence in face-centred cubic (FCC) crystals. Within a storage-recovery framework [1], the work hardening rate is obtained by combining the Taylor relation, which relates the stress to the density of stored dislocations, with an evolutionary law for the stored density. This evolutionary law allows estimating the net density resulting from dislocation storage and annihilation by dynamic recovery. The thermally activated character of this last process is usually thought to originate, for a large part, from the annihilation of screw dislocations by cross-slip. In this context, several current constitutive formulations derive from the one initially proposed by Teodosiu, Raphanel and Tabourot [2]. The parameters entering this type of model comprise the interaction strengths between slip systems that govern the flow stress, the mean free paths of dislocations, which govern the storage process and a recovery length, which is temperature- and strain rate-dependent [3]. The first two sets of parameters derive from elastic, mostly athermal, interactions of dislocations. Thus, they can be estimated from 3D dislocation dynamics simulations, as was done recently for the interaction strengths [4, 5]. It is not so for the recovery length, which is related to the annihilation properties of screw dislocations by cross-slip and, furthermore, depends on the unknown ratio of screw to edge dislocation densities in the microstructure.

Actually, it does not seem possible to rationalise all experimental results on the deformation of FCC single crystals by a single recovery length. Specifically, an examination of the existing experimental literature reveals that $<111>$ crystals exhibit an anomalously low rate of dynamic recovery, which is temperature and material dependent. Thus, the objectives

of the present work consist in understanding the mechanisms of this inhibited recovery and their relation with screw dislocation cross-slip and annihilation.

As shown in Section 2, the effect under investigation is clearly evidenced by comparing the stress-strain curves of <001> and <111> crystals and their temperature dependencies. The peculiarities of the <111> orientation were mentioned several times in the early literature. Kocks [6] indicated that in polyslip of single aluminium crystals, there are two extremely different types of behaviour, typified by <001> and <111> tension. In silver crystals, Ramaswami, Kocks and Chalmers [7] noted that the work hardening rate in crystals of <001> orientation decreases above the onset of dynamic recovery at a rate faster than in crystals of the <111> orientation, which is attributed to extensive cross-slip in <001> crystals. In addition, several studies [7-9] mentioned that the specific behaviour of <111> crystals is somehow related to the fact that the resolved applied stress in the cross-slip plane has a direction opposite to the one that favours the cross-slip process. This explanation is investigated in Sections 3 and 4, where two distinct causes for the inhibition of dynamic recovery are identified and examined. Both derive from the annihilation of screw dislocations of opposite sign in the particular state of stress that characterises the <111> orientation. The results are presented in terms of the relative ease of cross-slip and dislocation annihilation in <111> and <001> crystals. A concluding discussion is presented in Section 5.

2. Experimental aspects

This section focuses on a comparison between experimental shear stress - shear strain curves of <001> and <111> FCC crystals as a function of temperature. These curves present the characteristic features associated with multiple slip, especially an almost linear initial

slope followed by a pseudo-parabolic decrease of the strain hardening rate under the effect of dynamic recovery. The linear slope is akin to stage II of crystals initially oriented for single glide; it reflects the mostly athermal and material independent mechanism of dislocation storage. It is present in all deformation curves, but is practically reduced to an initial tangent at high relative temperatures, due to the onset of dynamic recovery. This last mechanism becomes significant beyond a more or less well-defined critical stress τ_{III}. The subsequent pseudo-parabolic strain hardening behaviour is strongly temperature and material dependent. It invades the whole stress-strain curve above a temperature that is correlated with the stacking fault energy (typically slightly above 300 K in Al, around 500 K in Cu, and at a somewhat higher temperature in Ag).

Figure 1 reproduces results obtained by Hosford, Fleischer and Backofen [10] on aluminium crystals between 4.2 K and 273 K. At the two lowest temperatures, the work hardening rate is larger for [001] crystals than for $[\bar{1}11]$ crystals. This is a common feature of the linear portion of the deformation curve in all FCC crystals. For a given stress, the work hardening rate is, as a rule, increasing with the number of active slip systems (see e.g. [11]). The stress-strain curves for the two types of crystals cross each other at 200 K. At 273 K, the [001] orientation exhibits a smaller strain hardening rate at all stresses, except perhaps at the onset of plastic flow. One finds similar deformation curves for aluminium at room temperature in [6] and in a review paper by Clarebrough and Hargreaves [12] (see fig. 27).

Fig. 1 about here

The same trend can be observed in copper single crystals, as illustrated by fig. 2, which reproduces experimental results by Kawasaki and Takeuchi [13] from 77 K to 873 K. In this case, there is always a cross over between the deformation curves of $[\bar{1}11]$ and [001] crystals

and the $[\bar{1}11]$ orientation is always harder at large strains. As temperature increases, the position of the cross over decreases toward smaller stress and strain values. The same feature is observed in another set of experiments performed in the same range of temperatures [11]. The reproducibility of the position of the cross over at room temperature can be checked from Göttler's work [14] (see fig. 1).

Fig. 2 about here

The same pattern of behaviour seems to be obtained in the case of silver crystals, although few stress-strain curves were published. From the results published by Mecking and Kocks [15] (see fig. 6) and Kocks and Mecking [1] (see fig. 31), one can infer that the strain hardening rate is larger for $<001>$ crystals than for $<111>$ crystals at room temperature and that dynamic recovery becomes more active in $<001>$ silver crystals than in $<111>$ crystals at higher temperatures.

Other experimental results confirm the peculiarities of the $<111>$ orientation. When an FCC single crystal is prestrained at low temperature and further restrained at a sufficiently high temperature, a drop in flow stress is recorded upon restraining. This work softening phenomenon was first investigated by Cottrell and Stokes [16]. Miura and Hamashima [9] further investigated work softening in aluminium between the prestrain temperature, 77 K, and 293 K. The orientations investigated were $<111>$, $<001>$ and a single slip orientation. Upon restraining, and after a transient, a significant drop in flow stress was recorded for the last two orientations. In parallel, slip trace analysis showed the occurrence of coarse slip lines and of extensive cross-slip activity. In contrast, the $<111>$ specimens did not exhibit work softening and the sample surfaces only showed traces of fine crystallographic slip. The authors concluded that work softening exhibits an orientation dependence that is controlled by

the aptitude to cross-slip. In these experiments, the drop in flow stress can be attributed to the sudden annihilation by cross-slip of the screw dislocations produced during the prestrain. These dislocations could not mutually annihilate at low temperature because dynamic recovery was not sufficiently active. Work-softening is particularly marked in aluminium crystals since most of the activation energy for cross-slip is furnished by thermal fluctuations at the restraining temperature. The particular behaviour of the <111> crystals, again, points out some inhibition of screw annihilations by cross-slip in this orientation.

Finally, in a publication by Miura and co-workers [8], it was shown that in silver crystals at room temperature, several characteristic resolved stresses become significantly larger close to the $<111>$ orientation than in other orientations. This concerns the stress τ_{III} for the onset of dynamic recovery on the stress-strain curves, but also the critical stress for twinning and the fracture stress, which all behave in the same manner. The orientation dependence of τ_{III} along the $<001>$ - $<111>$ boundary is reproduced in fig. 3. These τ_{III} values are reasonably well-defined in silver at 300 K, since they are much larger than the yield stresses (see fig. 31 of [1]).

Fig. 3 about here

From the examples given above, it appears that the inhibition of dynamic recovery and its temperature dependence are more spectacular and manifests themselves in a larger temperature range when one goes from aluminium to copper and silver, that is toward increasing dissociation widths. This strongly suggests interpreting the inhibition of dynamic recovery in $<111>$ FCC crystals in terms of an inhibition of the processes leading to the annihilation of screw dislocations by cross-slip.

3. Inhibited screw annihilations

It is generally accepted that the process of dynamic recovery "moves along" [1] with the formation of a dislocation cell structure. Jackson reviewed in some detail this parallel evolution [17], emphasizing the role of cross-slip and screw dislocation annihilations. Specifically, dynamic recovery is usually schematized as follows. A mobile dislocation reaches a dislocation wall and is blocked at some point by a stress field barrier. If a stored screw dislocation of opposite sign exists in the immediate neighbourhood, annihilation by cross-slip may occur. As these events occur in the complex structure of dislocation walls, only simplified estimates can be performed in somehow idealised configurations. Thus, we assume that the incoming screw dislocation is immobilized in its slip plane against a local stress barrier, in the immediate vicinity of the stored screw dislocation. Thus, the two attractive dislocations constitute a dipole, which is embedded into an internal stress field. Their relative positions depend on the local environment and the plane of the dipole should be non-crystallographic in the more general case.

In what follows, we only consider situations such that the incoming dislocation cross-slips and moves toward the stored dislocation. This motion occurs by a succession of slip and cross-slip events, during which interaction forces continuously increase. Nothing is known about the number and length of the glide steps, but this is not critical since what matters during the annihilation process is the interplay between the forces acting on the dislocations in the cross-slip planes. Thus, we define a generic configuration for annihilation by combining together all the cross-slip steps. The two screw dislocations are then set at the intersection of their slip planes with a common cross-slip plane, so that a single cross-slip event is needed to obtain annihilation (see fig. 5, below).

The forces or stresses discussed below result from the externally applied stress and the attractive interaction between the two screw segments. Annihilation occurs under the combined effect of these forces provided that the incoming dislocation can first cross-slip and then move in the cross-slip plane in the direction of the stored screw dislocation. The latter may be either mobile or immobile in its cross-slip plane. In what follows, it is assumed to be immobile, but the conclusions drawn below are valid in both cases. This is due to the fact that the inhibition rates are estimated in relative values for the two orientations [001] and $[\bar{1}11]$, so that possible correcting factors cancel out.

The stereographic plot of fig. 4 shows that the direction of the applied stress resolved in the cross-slip plane depends on specimen orientation.

Fig. 4 about here

We consider crystal orientations along the $[001]-[\bar{1}11]$ boundary, as in fig. 3. For the [001] orientation, the angle between the $[1\bar{1}1]$ normal to the cross-slip plane and the specimen axis is smaller than $\pi/2$. It reaches the value $\pi/2$ for the $[\bar{1}12]$ orientation, which has a null Schmid factor in the cross-slip plane, and is larger than $\pi/2$ for the [111] orientation. The angle between the active Burgers vector, $[\bar{1}01]$ and the slip plane normal is fixed. Thus, the direction of the applied stress resolved in the cross-slip plane changes sign when going from [001] to $[\bar{1}11]$. The consequences of this sign reversal on annihilations by cross-slip are shown in fig. 5. For each orientation of the stress axis, there are two possible configurations for mutual annihilation, depending upon whether the cross-slipping segment is above or below the stored one.

Fig. 5 about here

We examine first a single screw dislocation with a $1/2[10\bar{1}]$ Burgers vector, which is not part of a dipole. For a tensile stress axis along [001] or $[\bar{1}11]$, the resolved applied stress in the (111) slip plane, τ_{ag}, is acting along the direction parallel to the Peach-Koehler force, $[\bar{1}2\bar{1}]$. The direction of the resolved applied stress in the $(1\bar{1}1)$ cross-slip plane, τ_{acs}, is drawn from a straightforward calculation of the Peach-Koehler force. For the [001] orientation, τ_{acs} is acting along $[\bar{1}\bar{2}\bar{1}]$ (figs. 5 (*a*) and (*c*)), and the two consecutive directions of motion of a cross-slipping dislocation make an obtuse angle. This situation, which is commonly depicted in the literature, corresponds to *obtuse cross-slip*. For a $[\bar{1}11]$ stress axis, τ_{acs} is acting along [121] and the cross-slip direction makes an acute angle with the direction of motion in the slip plane (figs. 5 (*b*) and (*d*)). Thus, taking into account the sole effect of the applied stress, only *acute cross-slip* is permitted in the case of the $[\bar{1}11]$ orientation. There are a few mentions of acute cross-slip in the early literature. For instance Ramaswami, Kocks and Chalmers [7] discuss it in the case of $[\bar{1}11]$ silver crystals (see table 1 and fig. 10).

Consider now the additional effect of the interaction stress in the cross-slip plane (τ_{int} in fig. 5) with the screw dislocation of opposite sign. The two stresses acting in the cross-slip plane, τ_{acs} and τ_{int}, are anti-parallel in configurations (*b)* and (*c*) of fig. 5. Annihilation only occurs when the interaction stress prevails over the resolved applied stress in the cross-slip plane. We call this process *backward annihilation.* The two stresses are parallel in configurations (*a*) and (*d*), which corresponds to the familiar process of *forward annihilation*.

Furthermore, in configurations (*c*) and (*d*) of fig. 5, the projection of the interaction force on the slip plane is along the direction opposite to that of the resolved applied stress. This

reduces the glide stress that pushes the incoming dislocation against the obstacle and constricts it. As a consequence, the cross-slip probability is reduced (Section 4.2), with respect to configurations (a) and (b). This inhibiting factor is present in the two configurations such that annihilation can only occur in the acute direction of the cross-slip plane. In what follows, this process is called *acute annihilation*, by opposition to *obtuse annihilation*, in which the interaction stress favours the constriction process in the glide plane (figs. 5 (*a*) and (*b*)).

As a result, two distinct effects may inhibit annihilations by cross-slip. The first one is acute annihilation and the second one is backward annihilation. There is only one easy configuration for annihilation, obtuse annihilation, which occurs for a [001] stress axis (fig. 5 (*a*)). In what follows, it will be taken as reference. For each of the two configurations with a $[\bar{1}\,11]$ stress axis, annihilation may be inhibited for a different reason, backward annihilation or acute annihilation (figs. 5 (*b*) and (*d*)). For configuration (*c*), with a [001] stress axis, the two inhibiting processes are simultaneously present. Going from tension to compression changes the sign of the applied stresses in the slip and cross-slip planes but results in the same set of configurations for each orientation. Thus, no tension-compression asymmetry is predicted.

4. Estimates for the annihilation rate

Annihilation requires first that a cross-slip event occurs and next that the cross-slipped dislocation moves along the right direction. The objective is here to examine, in relative terms with respect to the [001] orientation, which of these mechanisms controls dynamic recovery in the $[\bar{1}\,11]$ orientation.

4.1. *Stresses and distances between dislocations*

The interaction stress, τ_{int}, is of the form $\tau_{int} = \mu b/2\pi d$, where d is the distance between the interacting screws. To investigate in dimensionless form the influence of this distance, we introduce a reference length scale $\ell = \rho^{-1/2}$, where ℓ is the average distance between dislocation segments in a microstructure containing a uniform density ρ of forest dislocations. Each the two orientations considered here has identical Schmid factors in the glide and cross-slip planes. With the help of the Taylor relation, the resolved applied stresses τ_{ag} and τ_{acs} (Section 3) can be written in the form $|\tau_{acs}| = |\tau_{ag}| = \alpha\mu b/\ell$, with $\alpha \approx 0.35$ [18]. Then,

$$\frac{|\tau_{acs}|}{|\tau_{int}|} = \frac{|\tau_{ag}|}{|\tau_{int}|} = 2\pi\alpha\frac{d}{\ell} \qquad (1)$$

In cell walls, the average distance between dislocations is smaller than ℓ. Therefore, a dislocation entering a cell wall interacts with nearest-neighbours at a distance d such that, in average, $d/\ell < 1/2$.

4.2. *Acute and obtuse annihilations*

In Escaig's model [19], the activation energy for cross-slip is of the form $\Delta G = \Delta G_o(1 - \beta\tau_g)$, where ΔG_o is the total activation energy and τ_g is the net glide stress pushing the perfect screw dislocation against the barrier in its slip plane. This linear stress dependence holds for $\tau_g < \Gamma/b$ (≈ 150 MPa in copper), where Γ is the stacking fault energy. The coefficient β depends on the resolved stresses on the partial dislocations in the slip and cross-slip planes (see equations (1) of [20, 21]). It leads to an orientation dependence of the cross-slip probability, the so-called Escaig effect [21], which however, does not come into play here (cf. fig. 2b of [21]). In addition, there is also no effect due to the interaction with the immobile

screw due the symmetry between acute and obtuse configurations. Therefore, the cross-slip probabilities for acute (*ac*) and obtuse (*ob*) annihilations are given by Arrhenius forms in which all coefficients, including the prefactors, are the same. This justifies writing the ratio r_{csp} of these probabilities for in the form

$$r_{csp} = \frac{P_{ac}}{P_{ob}} = \frac{\exp(V\tau_{gac}/kT)}{\exp(V\tau_{gob}/kT)}, \tag{2}$$

where k is the Boltzmann's constant and T the temperature. V is the activation volume, which is proportional to the square of the dissociation width under zero stress: $V \propto (d_o/b)^2$.

For obtuse annihilations (figs. 5 (*a*) and (*b*)), the glide stress τ_{gob} in the slip plane is $\tau_{gob} = \tau_{ag} + \tau_{int}\cos\theta$, where θ is the acute angle between the normals to the slip and cross-slip planes ($\cos\theta = 1/3$). In the case of acute annihilations (figs. 5 (*c*) and (*d*)), the effective stress in the slip plane is $\tau_{gac} = \tau_{ag} - \tau_{int}\cos\theta$. It favours cross-slip, with a reduced probability, provided that the glide stress is positive: $\tau_{int}/\tau_{ag} < \cos\theta$. From equation (1), this condition defines a critical value of d/ℓ, $(d/\ell)_c = \cos\theta/2\pi\alpha \approx 0.15$. Acute annihilations are only possible when the distance between the two screws is above this threshold value.

With the help of equation (1), the ratio of the cross-slip probabilities given by equation (2), is rewritten in the form:

$$r_{csp} = \frac{\sinh\left(\frac{\tau_{ag}}{S}\left(1 - \frac{\cos\theta}{2\pi\alpha}\frac{\ell}{d}\right)\right)}{\sinh\left(\frac{\tau_{ag}}{S}\left(1 + \frac{\cos\theta}{2\pi\alpha}\frac{\ell}{d}\right)\right)}, \tag{3}$$

where $S = kT/V$ is the strain rate sensitivity. Use is made of hyperbolic sines in order to account for inverse activation events occurring under small effective stresses near the threshold value [22]. This ratio is plotted in fig. 6 as a function of the dimensionless applied stress τ_{ag}/S for several values of d/ℓ larger than $(d/\ell)_c$.

Fig. 6 about here

We consider first the case of copper. From experimental data on the activation volume, the strain rate sensitivity is always slightly below or close to $S \approx 0.7$ MPa between 250 and 410 K and decreases outside this range [23, 24]. The ratio r_{csp} must be understood as the probability for acute annihilations in conditions such that the probability for obtuse annihilations is one. The resolved stress τ_{ag} must then be at least of the order of τ_{III} in [001] crystals, which is never less than about 30 MPa at temperatures below 400 K (fig. 2 and [13]). Hence, $\tau_{ag}/S \geq 40$, and one can see from fig. 6 that the probability for acute annihilation achieve non-vanishing values only when $d/\ell > 2$. As screw annihilations typically occur when $d/\ell < 1/2$ (Section 4.1), acute annihilations require rather unlikely local fluctuations in density and are practically forbidden. The same conclusion holds for materials with medium and large dissociation widths, like Ni, Ag and Au, where the strain rate sensitivity is similar to that of copper or larger. In aluminium, the dislocation core is narrow, so that the strain rate sensitivity is large and the total activation energy for cross-slip is small, as compared to copper. In addition, cross-slip is close to its athermal limit at this temperature, as manifested in fig. 2 by a sharp bent of the stress-strain curves shortly after the yield stress. From [23, 24], we have $S \approx 3.1$ MPa at 300 K and from fig. 1 and [10], we draw $\tau_{ag}/S = 2-3$ at 273 K and slightly more at 200 K. Then, Fig. 6 shows that for $(d/\ell)_c < d/\ell \leq 1/2$, acute annihilations can occur with a small but non-zero probability, typically between 0.05 and 0.15. Thus, in

contrast to other FCC crystals, acute annihilations are possible over a range of temperatures in aluminium, but with a small probability.

4.3. *Forward and backward annihilations*

We now examine the relative ease of forward (figs. 5(*a*) and (*d*)) and backward annihilations (figs. 5 (*b*) and (*c*)). The effective stresses in the cross-slip plane are denoted τ^*_f and τ^*_b, respectively. From fig. 5, we have $\tau^*_f = \tau_{int} + \tau_{acs}$ and $\tau^*_b = \tau_{int} - \tau_{acs}$. Making again use of equation (1), the ratios of the two effective stresses for forward and backward annihilations are rewritten:

$$\frac{\tau^*_f}{\tau_{acs}} = \frac{\tau_{int} + \tau_{acs}}{\tau_{acs}} = \frac{\ell}{2\pi\alpha d} + 1; \qquad \frac{\tau^*_b}{\tau_{acs}} = \frac{\tau_{int} - \tau_{acs}}{\tau_{acs}} = \frac{\ell}{2\pi\alpha d} - 1 \tag{4}$$

Backward annihilations are forbidden for small distances between the two screws, as they require interaction stresses larger than the applied stress, that is $d/\ell < 1/2\pi\alpha \approx 0.45$. A plot of these two dimensionless stresses as a function of the scaled distance between dislocations is shown in fig. 7.

Fig. 7 about here

The relative weight of forward and backward annihilations, $r_{bf}(d/\ell) = r_{ba}/r_{fa}$, can be estimated from fig. 7. For $0.2 < d/\ell < 0.45$, r_{bf} ranges between 0.4 and 0.06. Thus, backward annihilations are, indeed, impeded with respect to forward annihilations but are not vanishingly small. This conclusion derives from the consideration of a purely elastic process that is material-independent, not related to cross-slip probability and is not thermally activated.

In summary, dynamic recovery in [001] crystals essentially occurs by obtuse cross-slip and forward annihilations (fig. 5(*a*)). This is because the annihilation process depicted in fig. 5(*c*) requires the operation of two inhibited processes, acute cross-slip and backward annihilations. In $[\bar{1}11]$ FCC crystals with medium and large stacking fault energies, acute annihilation (fig. 5(*d*)) is practically forbidden. Obtuse annihilation with backward annihilation is possible (fig. 5(*b*)) and this last process is responsible for the inhibition of dynamic recovery. Aluminum, with its narrow dislocation core, may constitute an exception to this rule, as acute annihilations are permitted to some extent.

5. Discussion and concluding remarks

The present work relies on the assumption that the thermally activated nature of dynamic recovery and its material dependence can be treated in terms of the cross-slip mechanism. This view is, however, not unanimously accepted. One objection that is frequently raised is that dynamic recovery also involves the annihilation of non-screw dislocations (see [25] for discussion and references). According to recent studies [4, 26], the annihilation of non-screw segments can locally occur by the interaction of dislocations of same Burgers vectors lying in their slip and cross-slip planes. These so-called collinear annihilations concern a wide range of non-screw orientations. However, they occur in a purely mechanical manner and do not contribute to the global process of dynamic recovery. Thus, we feel it justified to treat the latter in terms of the annihilation of screw dislocations by cross-slip.

For the present purposes, which involved simple considerations, cross-slip was treated using the Escaig's model. A specific model for the annihilation of screw dipoles by cross-slip, which extends Hirsch's jog model for cross-slip [27], was developed by Brown [28]. In the

practice, Brown's model should not lead to conclusions different from those obtained here (M. Brown, private communication).

Two main causes for the inhibition of screw dislocation annihilations were investigated, acute annihilations and backward annihilations. In FCC crystals, with the notable exception of aluminium, the inhibition of dynamic recovery is governed by backward annihilations. As this process is athermal, the dynamic recovery length is reduced by a constant factor when going from [001] to $[\bar{1}11]$, whatever the temperature. In aluminium, due to the narrow dislocation core, acute annihilations may also occur with a reduced rate and within a finite range of temperatures. This makes the modelling of dynamic recovery more challenging in this material. Consequences regarding strain hardening will be discussed in a separate study. Acute cross-slip occurs in 3D dislocation dynamics simulations and tests on dislocation annihilations at low applied stresses are in progress.

In materials with crystallographic structures other than FCC, dynamic recovery may be inhibited for one or several particular orientations. The distinction between obtuse and acute annihilation only vanishes when the slip and cross-slip planes are at right angles. However, backward annihilations are always present when the slip geometry is such that the direction of the resolved stress in the cross-slip plane changes sign within the standard stereographic triangle.

In conclusion, the sign reversal of the resolved applied stress in the cross-slip plane explains the significant differences that were recorded a few decades ago in the mechanical response of $<001>$ and $<111>$ crystals. This phenomenon, which is not mentioned in the current literature, is also important for the modelling of polycrystals. Indeed, in that case, the

mechanical behaviour of most of the individual grains is similar to that of single crystals with $<001>$ and $<111>$ orientations [6, 29].

Acknowledgements

The authors are indebted to Dr. W. Pantleon for drawing their attention to the inhibition of cross-slip in $<111>$ crystals. Helpful discussions with Prof. J. Bonneville and Dr. U.F. Kocks are gratefully acknowledged.

References

[1] U.F. Kocks and H. Mecking, Progr. Mat. Sci. **48** 171 (2003).

[2] C. Teodosiu, J.L. Raphanel and L. Tabourot, in *Large Plastic Deformations*, edited by C. Teodosiu, J.L. Rapahanel and F. Sidoroff (A.A. Balkema, Rotterdam, 1993), p 153.

[3] U.F. Kocks, J. Eng. Materials and Eng. Technol. **98** 76 (1976).

[4] R. Madec, B. Devincre, L. Kubin, T. Hoc and D. Rodney, Science **301** 1879 (2003).

[5] B. Devincre, L. Kubin and T. Hoc, Scripta mater., in press.

[6] U.F. Kocks, Acta metall. **8** 345 (1960).

[7] B. Ramaswami, U.F. Kocks and B. Chalmers, Trans AIME. **233** 1632 (1965).

[8] S. Miura, J. Takamura and N. Narita, Trans. JIM Supplement **9** 555 (1968).

[9] S. Miura and K. Hamashima, J. Mater. Sci. **15** 2550 (1980).

[10] W.F. Hosford, R.L. Fleischer and W.A. Backofen, Acta metall. **8** 187 (1960).

[11] T. Takeuchi, Trans JIM **16** 629 (1975).

[12] L.M. Clarebrough and M.E. Hargreaves, Progr. Metal. Phys. **8** 1 (1959).

[13] Y. Kawasaki and T. Takeuchi, Scripta metall. **14** 183 (1980).

[14] E. Göttler, Phil. Mag. **28** 1057 (1973).

[15] H. Mecking and U.F. Kocks, Acta metall. **29** 1865 (1981).

[16] A.H. Cottrell and R.J. Stokes, Proc. Roy. Soc. **A233** 17 (1956).

[17] P.J. Jackson, Progr. Mat. Sci. **29** 139 (1985).

[18] J. Gil Sevillano, in *Plastic Deformation and Fracture of Materials*, edited by H. Mughrabi (VCH, Weinheim, 1993), p. 19.

[19] B. Escaig, in *Dislocation Dynamics*, edited by A.R. Rosenfeld, et al., (McGraw-Hill, New York, 1968), p. 655.

[20] J. Bonneville, B. Escaig and J.L. Martin, Acta metall. **36** 1477 (1988).

[21] J. Bonneville and B. Escaig, Acta metall. **27** 1989 (1979).

[22] U.F. Kocks, A.S. Argon and M.F. Ashby, Progr. Mat. Sci. **19** 1 (1975).

[23] D. Caillard and J.L. Martin, *Thermally Activated Mechanisms in Crystal Plasticity* (Pergamon-Elsevier, Amsterdam, 2003).

[24] J. Bonneville and G. Vanderschaeve, in *Strength of Metals and Alloys*, edited by H.J. McQueen et al. (Pergamon Press, Oxford, 1986), Volume 1, p. 9.

[25] F.R.N. Nabarro, in *Strength of Metals and Alloys*, edited by H.J. McQueen et al. (Pergamon Press, Oxford, 1986), Volume 3, p. 1667.

[26] B. Devincre, T. Hoc and L. Kubin, Mat. Sci. Eng A **400-401**, 182 (2005).

[27] P.B. Hirsch, Phil. Mag. **7** 67 (1962).

[28] L.M. Brown, Phil. Mag. A **82** 1691 (2002).

[29] N. Hansen and X. Huang, Acta mater. **46** 1827 (1998).

Figure captions

Figure 1. Shear stress - shear strain curves of $[\bar{1}11]$ and [001] aluminium crystals between 4.2 K and 273 K. For clarity, the curves are shifted horizontally by a constant value (Redrawn from [10]).

Figure 2. Shear stress - shear strain curves of $[\bar{1}11]$ and [001] copper crystals between 77 K and 873 K (Redrawn from [13]).

Figure 3. Orientation dependence of the stress τ_{III} for the onset of stage III in silver crystals at 300 K. ϕ is the angle between the [001] orientation and other orientations along the $[001]-[\bar{1}11]$ boundary. After Miura, Takamura and Narita [8].

Figure 4. The geometry of cross-slip in the standard stereographic plot. The primary slip system is $[\bar{1}01](111)$ and the cross-slip system is $[\bar{1}01](1\bar{1}1)$. The Schmid factor in the cross-slip plane, F_{CS}, vanishes along the $[011]-[\bar{1}12]$ boundary, as the normal to the $(1\bar{1}1)$ plane is perpendicular to the loading axis.

Figure 5. An incoming screw dislocation (+) interacting with an immobile dislocation of opposite sign (-). The configurations for crystals deformed along [001] and $[\bar{1}11]$ stress axes, are shown respectively in the left and right columns. The two consecutive arrows represent the directions of the applied stresses on the (+) dislocation, resolved in the slip and cross-slip planes. τ_{int} is the interaction stress acting along the direction of the attractive interaction force in the cross-slip plane. Configurations (*a*) and (*c*) correspond to obtuse cross-slip and

configurations (*b*) and (*d*) to acute cross-slip. Forward annihilations occur in configurations (*a*) and (*d*) and backward annihilations in configurations (*b*) and (*c*).

Figure 6. The ratio of cross-slip probabilities for acute and obtuse annihilations as a function of the resolved applied stress in the slip plane τ_{ag}, scaled by the strain rate sensitivity S. This ratio is drawn for several values of the distance between the two attractive dislocations above the threshold value $(d/\ell)_{\min} = 0.15$.

Figure 7. The effective stresses for forward (*fa*) and backward (*ba*) annihilations, scaled by the resolved applied stress in the cross-slip plane, τ_{acs}, as a function of the scaled distance d/ℓ between the interacting screw dislocations. Backward annihilation can only occur below the threshold value $1/2\pi\alpha$.